Journal of the Korean Physical Society, Vol. 50, No. 5, May 2007, pp. 1290∼1293

Quantization of the Current Induced by a Surface Acoustic Wave through a Quantum Point Contact

Nam Kim, Byung-Chill Woo and Jinhee Kim
Dicision of Advanced Technology, Korea Research Institute of Standard and Science, Daejeon 306-600

Minky Seo and Yunchul Chung*
Department of Physics, Pusan National University, Busan 609-735

(Received 26 February 2007)

The acousto-electric currents through a quantum point contact induced by surface acoustic waves were observed. The current was found to be quantized at integer multiples of ef, where f is the surface acoustic frequency. By using an interdigitated transducer with a 500 nm spacing between the gates, we produced surface acoustic waves at 2.456 GHz, which resulted in 1.18 nA quantized current when three electrons were transferred from the source to the drain at a time. Also, we found that the quantization is related to the a presence of a static quantum dot unintentionally formed in a quantum point contact.

PACS numbers: 73.50.Rb, 73.40.Gk, 73.23.Ad
Keywords: Current standard, Surface acoustic wave, Quantum dot, Quantum point contact

I. INTRODUCTION

The standard for current has not been changed since the first establishment of a current standard defined by the Biot-Savart Law [1]. Recently, the charge pump, which transfers electrons one by one between two electrodes at zero bias, has become the most promising candidate for a quantum current standard [2–5]. In pumping, an external ac electric field can generate a dc current, $I = nef$, where e is the electronic charge, n is the number of electrons transferred per cycle, and f is the frequency of the external ac potential. Until now, two types of charge pumps have been realized: a Coulomb-blockade (CB)-based charge pump composed of metallic islands [3,4] or qunatum dots (QD) [6–8] and a surface-acoustic-wave (SAW)- driven pump [9–11]. However, the CB-based charge pump has to work at rather lower frequencies to insure the high probability of tunneling events so that the resulting current is accurate enough as a current standard. Also, the relatively long RC time constant of the circuit limits the operating frequency. Usually, the operating frequency is limited to a few tens of MHz, and this results in a few pA output current. Such a current is difficult to measure precisely and is difficult to compare with an unknown current that needs to be calibrated. On the other hand, the SAW-driven pump can produce a relatively large current by delivering surface acoustic waves through a quasi 1-D conduction channel. Conventionally, a 1-D conduction channel is fabricated using a 2-D electron gas system based on AlGaAs-GaAs hetero-junction [9–11]. Quite recently, there have been new attempts to use carbon-nanotubes as 1-D conduction channel [12,13].

When the SAW is applied on the surface of the device, the electric field induced by the SAW changes the conduction band energy profile locally. This modulates the conduction band energy profile to a sinusoidal shape in the direction of the SAW propagation. When the SAW enters the constriction formed by a quantum point contact (QPC), which forms a quasi-1D conduction channel parallel to the direction of the SAW propagation, the superposition of the SAW-induced potential and the conduction band profile of the QPC forms a moving quantum dot. Since the number of electrons inside a quantum dot is quantized by integer numbers, this scheme allows one to transfer an integer number of electrons per single SAW cycle. Hence the transferred current becomes $I = nef$, where f is the frequency of the surface acoustic wave and n is the number of electrons inside the moving quantum dot. The advantage of this method is that the operating frequency is not limited by the RC time of the device. Since it is not so difficult to create SAW at a few GHz range, one can easily get around 1 nA of output current, which is more practical as a current standard. In this paper, we demonstrate the fabrication and the operation of such a SAW-driven charge pump.

*E-mail: ycchung@pusan.ac.kr; Fax: +82-51-513-7664

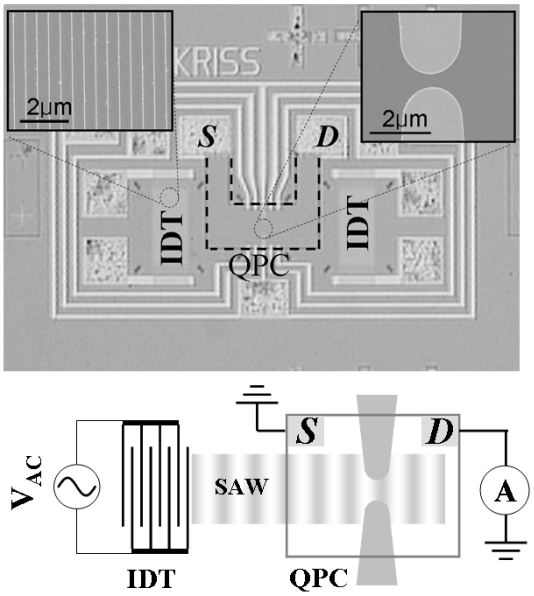

Fig. 1. Picture of the device taken by using an optical microscope. The SEM picture of the IDT and the QPC are shown in the left and the right inset, respectively. The individual gate for the IDT is 300 μm long and 50 nm wide, and 240 repetitions are made at every 500 nm to make a 300 μm by 120 μm IDT. The dashed lines are drawn on the edge of the mesa for clarity. The source and the drain are marked by S and D, respectively. The bottom figure is a schematic diagram of our device.

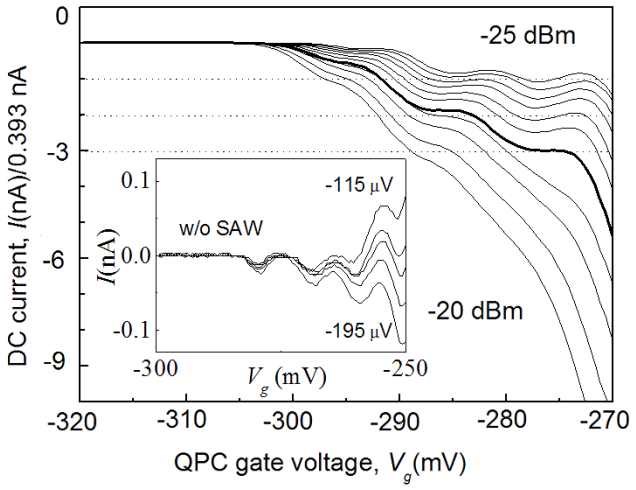

Fig. 2. Acousto-electric current as a function of the QPC gate voltage at different SAW power levels. The bias was set to –155 μV. The SAW power levels were –25 dBm to –20 dBm in steps of –0.5 dBm from top to bottom. The dashed lines are guide lines for 0.393 nA (ef at 2.456 GHz, which is the resonant frequency of the SAW transducer), 2 × 0.393 nA, and 3 × 0.393 nA. The thick line shows well developed 2nd and 3rd plateaus which is measured at the SAW power of –22 dBm. The inset shows the output currents as a function of the QPC gate voltage at various bias voltages. No surface acoustic wave is applied to the device. The bias voltages are –195 μV, –175 μV, –155 μV(thick line), –135 μV, and –115 μV from bottom to top.

II. EXPERIMENT AND DISCUSSION

The device consists of mainly two parts as it is shown in Figure 1. One is a quantum point contact(QPC), which is used to form a quasi-one-dimensional conduction channel, and the other is an inter-digitated transducer (IDT) to produce the SAW. An SEM picture of the fabricated QPC is shown in the right inset of the figure. The width of the straight part of the QPC was around 2 μm while the smallest gap between the gates was around 500 nm. The left inset of the figure is an SEM picture of the inter-digitated transducer. To generate a 1 μm long SAW, we kept the spacing between the gates at 500 nm and each gate was 50 nm wide and 300 μm long. The devices were fabricated on the surface of an 80 nm deep 2-dimensional electron gas (2DEG) layer based on a GaAs/AlGaAS heterostructure with an electron density of 2×10^{11} cm^{-2} and a mobility of 2×10^{6} cm^{2}V^{-1}s^{-1} at 4.2 K. First, the mesa was defined by etching away the unnecessary 2DEG layers in a $H_2O_2 : H_3PO_4 : H_2O$ (1 : 1 : 50) solution, which gave an etch rate of around 100 nm/s at room temperature. For the ohmic contact to the 2DEG of the mesa, 30 Å of Ni, 2000 Å of Au, and 1000 Å of Ge, followed by 750 Å of Ni, were evaporated and annealed at 460 °C for 60 seconds. The QPCs were fabricated by using electron beam lithography. 200 k 3% PMMA in anisole followed by 495 k 5% PMMA in anisole were coated to form a double e-beam resist layer to make lift-off easier and to give good enough resolution for very fine structure fabrications. Thermal evaporation of 150 Å of Ti to form a good Schottky contact with 2DEG and 150 Å of Au were put on top of the Ti layer to prevent oxidation of Ti and to give good electrical contact to later process layers. After the fabrication of the QPC, an IDT was fabricated with the same e-beam lithography process, but with a different metal deposition. It is important to make IDT gates as light as possible otherwise, the surface acoustic wave can be attenuated by the IDT gates themselves while the SAW is propagating under the IDT gates. We used 50 Å of Ti for the Schottky contact with the 2DEG, and 300 Å of Al to reduce the weight of the gate and another 50 Å of Ti and finally 50 Å of Au to prevent oxidation. As we mentioned, a Ti layer was sandwiched between the Al and the Au layers to prevent so called purple plague, which is an intermetallic compound of aluminium and gold. The purple plague is widely known to cause a bad electric connection between the Al and the Au layers. Finally, large electrical contact pads were fabricated with optical lithography.

The measurements were done at $T = 2$ K in a variable temperature insert. Semi-rigid coaxial cables were installed on the insert to deliver microwave signals for the IDT. The inset of Figure 2 shows the DC output current

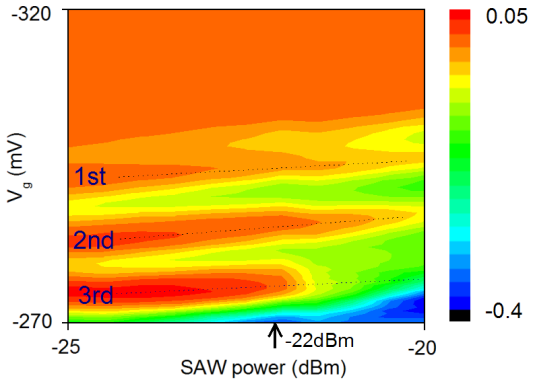

Fig. 3. Pseudo-color plot of the transconductance (dI/dV_g) taken at various SAW powers and QPC gate voltages.

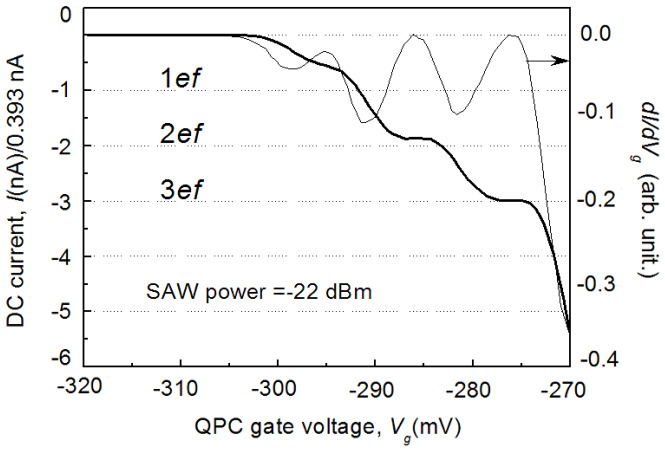

Fig. 4. Quantization of currents as a function of the QPC gate voltage for a SAW power of –22 dBm was delivered to the IDT (thick solid line). The dashed horizontal lines are guide lines for $I = ef$, $2ef$, and $3ef$. The transconductance, the numerical derivative of the current with respect to the gate voltage, is plotted as a thin solid line. The transconductances become zero for the second and the third plateaus.

as a function of the QPC gate voltage at various bias voltages, in the absence of a SAW. It shows CB-like oscillations that depend on the gate voltages at finite bias voltages. This current oscillation reflects the dependence of the gap energy modulation on the gate voltages (not shown here). The gap size was measured to be about 2 – 3 meV. If this energy gap is assumed to be due to the CB of the QD formed inside the QPC, the size of the static QD is estimated to be about 0.2 to 0.3 μm [14]. It is well known that a quantum dot can be formed inside a relatively long QPC due to the perturbation of the potential landscape of a 1-D wire by impurity states [14,15]. According to the data in the inset of Figure 2, there exists a dc bias offset of approximately -155 μV. Usually, there can be some unwanted DC bias applied across the sample due to the thermo-electric voltage developed between the electric wires used for the measurement. Such a thermo-electric voltage can shift the zero-current voltage away from zero bias. In order to minimize the offset dc current induced by the thermo-electric voltage, we set the dc bias voltage to -155 μV in the following SAW-induced current measurements. However, even for an effectively zero bias voltage, at -155 μV there still exists CB oscillations. It is not clear where the extra dc current comes from.

Figure 2 shows the response of the DC output currents to the surface acoustic waves as a function of the SAW power, where we have used a resonant frequency of 2.456 GHz [16]. It can be clearly seen that the CB peaks are evolving into a current plateau as the SAW power is increased. Figure 3 shows a 2-dimensional density plot of the transconductance dI/dV_g as a function of the SAW power and the gate voltages, V_g. It shows that the 1st, 2nd, and 3rd peaks of the CB evolve into the 1st, 2nd, and 3rd current plateaus as power increases, where the current plateaus can be defined by $dI/dV_g = 0$ and are denoted by an orange color. Contrary to the authors' observations [14], the area of current plateaus in the parameter space spanned by gate voltage V_g and the SAW power is relatively small. For instance, the three plateaus never show up at the same time. However, the 2nd and the 3rd plateaus develop simultaneously at the same SAW power of around –22 dBm, as denoted by the arrow in Figure 3. This is a very unique feature. Even though the power window is very narrow, quantized current steps are revealed at the same SAW power of –22 dBm. The transconductance becomes zero at the second and the third plateaus in Figure 4. The 3rd current plateau shows the $I = 3ef$ relation while the value of the second plateau is less than expected and the first plateau is not well established. These features are far from the conventional SAW-induced current in QPC devices [9–11] where the quantized electrons transferred by the moving quantum dot formed by the SAW potential superposed on the QPC potential barrier. Our case is more analogous to the observations reported by the authors [14] from the following point of view. First, we observed a quantized current through a static QD unintentionally formed in a QPC. Secondly, the CB oscillation peaks evolved into quantized current plateaus. Thirdly, a so called *fractional plateau* was observed for the first plateau, whose origin is not known yet. The authors [14] attributed the quantized current to a turnstile operation of a static QD embedded inside a QPC: the SAW worked simply as phase-shifted AC voltage on the quantum dot gates, hence enable the quantum dot to work as a turnstile for electrons [14,17]. However, the simple turnstile pumping model cannot explain our observation that the 2nd and the 3rd current plateau are observed simultaneously only in the narrow window of a SAW power around –22 dBm. Unlike the size of the QD of Ref. 14, the size of our QD was estimated to be approximately from 0.2 μm to 0.3 μm, which is much smaller than the 1 μm wavelength of the SAW. This means that the phase of the SAW did not match well with the size of the QD. Thus,

we cannot explain our observations only with the simple turnstile pumping model. In order to explain our features, we need further study on the QD-embedded QPC system, where the wavelength of the SAW is longer than the size of a QD and the width of the QPC potential barrier is comparable to the size of a static QD.

III. CONCLUSIONS

The current quantization induced by a SAW coupled to a static quantum dot inside a QPC has been demonstrated. The maximum quantized current was 1.1752 nA at a SAW frequency of 2.456 GHz which corresponds to a transfer of three electrons per SAW cycle. The deviation of the quantized current from the expected value was less than 0.3 %. We could not explain our observations simply in terms of either a turnstile mode or conventional SAW-induced pumping through a QPC. In order to explain our observations, we need further study of the QD embedded QPC system, where the wavelength of the SAW is longer than the size of a QD and the width of the QPC potential barrier is comparable to the size of a static QD.

ACKNOWLEDGMENTS

This work was supported by a Korea Research Foundation Grant(KRF-2004-003-C00076). The ampere was defined in the 9th General Conference on Weights and Measures (Paris, 12-21 October 1948).

REFERENCES

[1] *The Ampere was Defined in the 9th CGPM* (the General Conference on Weights and Measures, 1948).
[2] F. Cuinea and N. Garcia, Phys. Rev. Lett. **65**, 281 (1990).
[3] L. J. Geerligs *et al.,* Phys. Rev. Lett. **64**, 2691 (1990).
[4] M. W. Keller *et al.,* Appl. Phys. Lett. **69**, 1804 (1996).
[5] D. Esteve, *Single Charge Tunneling* (Plenum, New York, 1992), Chap. 3.
[6] A. Fujiwara *et al.,* Appl. Phys. Lett. **84**, 1323 (2004).
[7] J. H. Kim *et al.,* J. Korean Phys. Soc. **45**, S585 (2004).
[8] L. P. Kouwenhoven *et al.,* Phys. Rev. Lett. **67**, 1626 (1991).
[9] V. I. Talyanskii *et al.,* Phys. Rev. B **56**, 15180 (1997).
[10] J. Cunningham *et al.,* Phys. Rev. B **60**, 4850 (1999).
[11] J. Cunningham *et al.,* Phys. Rev. B **62**, 1564 (2000).
[12] P. J. Leek *et al.,* Phys. Rev. Lett. **95**, 256802 (2005).
[13] Y.-S. Shin *et al.,* Phys. Rev. B **74** 195415 (2006).
[14] N. E. Fletcher *et al.,* Phys. Rev. B **68**, 245310 (2003).
[15] D. Chang *et al.,* J. Korean Phys. Soc. **49**, 692 (2006).
[16] The negative sign of the induced currents was purely due to the configuration of the measurement circuit. By reversing the SAW direction, induced currents were changed to positive.
[17] A. A. Odintsov, Appl. Phys. Lett. **58**, 2695 (1991).